Image Stitching of PCBs for Reverse Engineering and Metrological Application

Simran Pal Singh Bawa *simranpalsingh24@gmail.com*
Department of Mechatronics
SRM University
Chennai, 603203, India

Abstract

This paper addresses the solution towards the problem of lacking CAD data of the PCBs for repair and reverse engineering industries. In this work, concept of image mosaicking is employed. Where special distortion free optics is used to acquire images of the PCB and later theses images are stitched together to extract the pads location. Stitching Algorithm here incorporates the use of Harris corner detection for the extraction of interest points and then using popular RANSAC algorithm for the identification of the correspondence points. One of the novelty of this algorithm is the design and use of the correspondence point filter, which allows only the best match points to pass and contribute for homography matrix. Second novelty is the skew correction of the final stitched image for enhancing the accuracy.

Keywords: Image Mosaicking, Correspondence Point Filter, Harris Corner Detector, Rigid Transformation, Radial Distortion, Image Registration.

1. INTRODUCTION

Achieving high accuracy in image stitching has always been a challenge. Image mosaicking in the field of computer vision has a variety of applications in satellite imagery and photogrammetry. The main reason behind the need of image mosaicking is limited vision span of a camera, unlike human vision which is up to 200 degree [1]. Image stitching is followed by image registration. Image Registration is responsible for the establishment of the correspondence points between two images. These two images are acquired from a different point of view and they share some common region. Image Registration consists of feature detection, feature matching, and transform model estimation. In image stitching, features extraction refers to computing abstraction of the image information. This information is in the form of isolated points used as a subset of the image domain[2]. Various techniques to extract feature points are: Harris corner detection, Foerstner corner detection, SIFT etc. But Harris is the most robust among all these. It is discussed in section 6.1. For feature matching and transform model estimation RANSAC is used. Discussed in section 6.2. Implementation of generating a highly accurate PCB Mosaic is discussed in section 8 followed by limitations and conclusion.

2. PROBLEM STATEMENT

In the field of electronics reverse engineering and servicing industry, repair and functional testing is carried out by using flash programming or boundary scan, frequency and other measurements. Now a days mostly for these boards in-circuit test (ICT) fixtures or flying probes are used. Generally they require CAD file of the PCB for the fixture designing in ICT testing method or for high accuracy landing of probing needle on small pads using flying prober. But due to the lack of CAD data of the board, repair or redesign becomes extremely slow and inaccurate. This paper presents a technique to overcome this problem. Our goal is to take multiple images of the PCB and stitch them together to obtain highly accurate location information of the test points.

3. CAMERA CALIBRATION

Camera Calibration is one of the most important and first step towards any machine vision application. This calibration process is carried out with the help of a calibration plate. These calibration plates consist of features and dimensions which are already know to image processing software, and therefore with the help of prescience knowledge, software is able to determine the pose and lens distortion correction coefficients.

3.1 Lens Distortion – Radial type

Distortions are aberrations in an optical system which can be caused due to the shape of the lens itself or positioning of the optical elements. These aberrations can be irregular or may follow radially symmetric patterns such as barrel distortion or pincushion distortion [3]. Because of these aberrations the reproduced image consists of several anomalies.

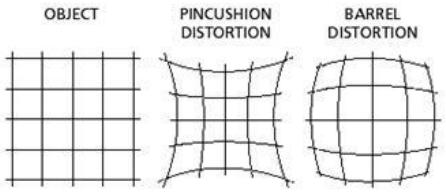

FIGURE 1 (A) (B) (C).

Barrel Distortion as shown in figure 1(c) leads to reduction in image magnification with respect to the distance from the optical axis. Pincushion distortion as shown in figure 1(b) tends to increase the image magnification with respect to the distance from the optical axis.
This type of distortion can be rectified using Brown's Distortion Model [4].

$$x_{\mathrm{d}} = x_{\mathrm{u}}(1+K_1r^2+K_2r^4+\cdots)+(P_2(r^2+2x_{\mathrm{u}}^2)+2P_1x_{\mathrm{u}}y_{\mathrm{u}})(1+P_3r^2+P_4r^4+\cdots) \quad (1)$$

$$y_{\mathrm{d}} = y_{\mathrm{u}}(1+K_1r^2+K_2r^4+\cdots)+(P_1(r^2+2y_{\mathrm{u}}^2)+2P_2x_{\mathrm{u}}y_{\mathrm{u}})(1+P_3r^2+P_4r^4+\cdots) \quad (2)$$

Where:

$(x_{\mathrm{d}},\ y_{\mathrm{d}})$ = axis image point as projected on image plane using specified lens,

$(x_{\mathrm{u}},\ y_{\mathrm{u}})$ = Undistorted image points as projected by an ideal pin-hole camera,

$(x_{\mathrm{c}},\ y_{\mathrm{c}})$ = Distortion center,

$K_n = n^{\mathrm{th}}$ = Radial Distortion Coefficient,

$P_n = n^{\mathrm{th}}$ = Tangential Distortion Coefficient,

$r = \sqrt{(x_{\mathrm{u}}-x_{\mathrm{c}})^2+(y_{\mathrm{u}}-y_{\mathrm{c}})^2}$, and

... = an infinite series.

Correction of these distortions can be done by wrapping the image with its opposite distortion. Generally, Barrel distortion yields a negative term of K_1 and Pincushion yields a positive value.

3.2 Lens Distortion – Perspective Type

When wrapping or transformation of an object differs drastically from what the object appears from a normal focal length then it is called as perspective distortion. This occurs due to the relative distance at which the image is captured and the angle of view of the image. This type of distortion is very common in wide angle lenses and it reduces with the increase of focal length. Figure 2(a) and (b) depicts perspective distortion.

FIGURE 2(a).

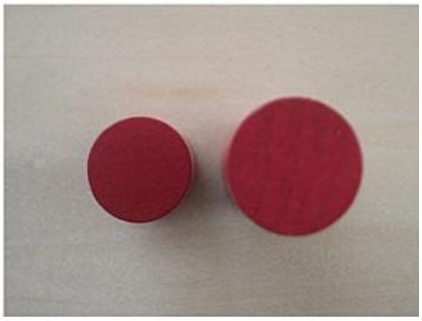

FIGURE 2(b).

Telephoto lenses are the solution to eliminate such perspective error. Ideally, super telephoto lenses have their entrance pupil at infinity and this produces an orthogonal view of the object [5]. As shown in figure 3.

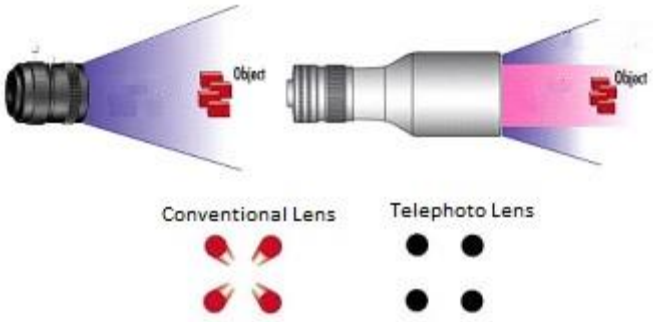

FIGURE 3: Orthogonal view from conventional lens Vs telephoto lens.

4. IMAGE ACQUISTION RULES

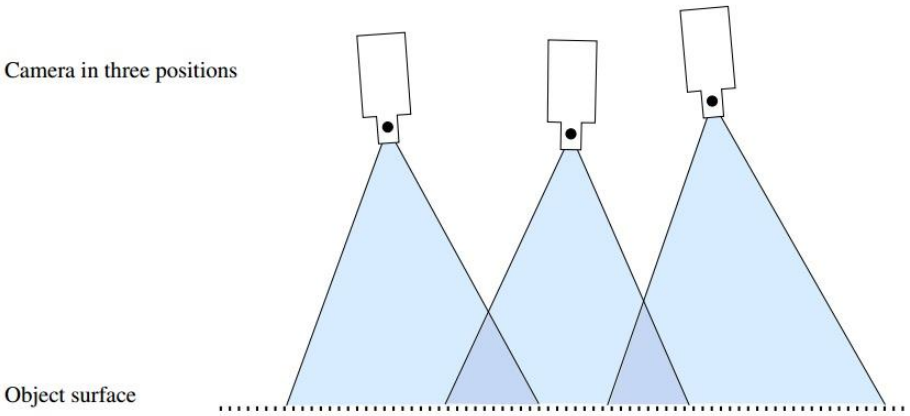

FIGURE 4: Image Acquisition Technique.

As shown in the figure 4 image mosaicking between two images is possible only when both the images share some percentage of common area or overlapping region. Also, It is important to have texture in the images in order to identify correct interest points. Generally an overlapping area of 10-20% is good. If the images are not taken from a telephoto lens then distortion correction must be done first. The images must be radiometrically similar otherwise seam between the images will be visible clearly. Any suitable entocentric lens can be used for imaging

when dealing with flat objects e.g Bare PCB. But for the stitching of an assembled PCB a telephoto lens with sufficient depth of field should be used to avoid parallax error. It is also important to make sure that during the capturing process neither the camera nor the PCB should be rotated around the optical axis. It is also advised to have a constant FOV throughout the capturing process. This can be done by keeping a constant Working Distance between PCB and Lens [6].

5. TRANSFORMATION MATRIX

A transformation matrix shows how a perceived object changes as the observer's view point changes. Linear transformation can be easily represented by matrices. In 2D graphics, most common geometric transformations are Rotation, Scaling, Reflection, and orthogonal projection.

5.1 Rotation Matrix

For a rotation about the origin by angle θ in clockwise direction the linear algebraic form is x' = xcos θ + ysin θ and y' = -xsin θ + ycos θ [7]. The matrix form can be written as:

$$\begin{bmatrix} x' \\ y' \end{bmatrix} = \begin{bmatrix} \cos\theta & \sin\theta \\ -\sin\theta & \cos\theta \end{bmatrix} \begin{bmatrix} x \\ y \end{bmatrix}$$

5.2 Shearing Matrix

Shearing can be done along both x and y axis. A shear parallel to x axis has x' = x + ky and y' = y. Where as a shear parallel to y axis has x' = x and y' = y + kx. Further discussed in Section 7

$$\begin{bmatrix} x' \\ y' \end{bmatrix} = \begin{bmatrix} 1 & k \\ 0 & 1 \end{bmatrix} \begin{bmatrix} x \\ y \end{bmatrix}. \qquad \begin{bmatrix} x' \\ y' \end{bmatrix} = \begin{bmatrix} 1 & 0 \\ k & 1 \end{bmatrix} \begin{bmatrix} x \\ y \end{bmatrix}$$

5.3 Affine Transformation

Homogenous coordinates are used to represent affine transformation. This means that a 2-vector(x,y) can be written as a 3-vector(x,y,1). Using a 2D affine transformation matrix all the above geometric transformation can be performed [8].

$$\begin{bmatrix} \cos\theta & \sin\theta & t_x \\ -\sin\theta & \cos\theta & t_y \\ 0 & 0 & 1 \end{bmatrix}$$

Here, elements of location A_{11}, A_{12}, A_{21}, A_{22} are responsible for rotation and scaling. Elements on location A_{13}, A_{23} are responsible to translation in x and y axis respectively. The last row has elements A_{31}, A_{32}, A_{33} which are projective vectors and for affine transformation their values are 0, 0 and 1 respectively. The accuracy of image stitching is highly dependent of this matrix.

6. PROPOSED ALGORITHM

6.1 Harris Corner Detector

Due to strong invariance [9] to image rotation, scale, illumination and view point changes, Harris Corner Detection [10] is a very robust interest point detector. This is mainly because of its computation in the first order derivative of the image. A distant approach to Harris corner detector was presented by Marovac [11], where a local window in the image is shifted by small amount in various directions and corresponding average changes in the image intensity are determined. There intensity values can fall in following three cases:

1. If the intensities are approximately constant which means that window is in a flat region.
2. If the window falls on a edge then a significant change in the intensity will be observed while shifting along the direction perpendicular to the edge.

3. If the window falls on a corner, then large changes in the intensity will be observed while shifting along the direction of the edge.

Harris Operator [12] is based on the smoothed matrix M.

$$M = G_\sigma * \begin{pmatrix} \sum_{c=1}^{n} I_{x,c}^2 & \sum_{c=1}^{n} I_{x,c} I_{y,c} \\ \sum_{c=1}^{n} I_{x,c} I_{y,c} & \sum_{c=1}^{n} I_{y,c}^2 \end{pmatrix}$$

Here G_σ is the Gaussian smoothing of size σ. $I_{x,c}$ and $I_{y,c}$ are the first derivative of the image channel using a Gaussian convolution of size sigma grade. Positive local points are defined by the following equations.

$$R = Det(M) - Alpha*(TraceM)^2 \quad .....(3)$$

$$R = \lambda_1 \lambda_2 - K (\lambda_1 + \lambda_2)^2 \quad .....(4)$$

Here, R is depends on a constant K and value for K can be in a range from 0.001 to 0.1

6.2 RANSAC

Random Sample Consensus [13] an algorithm for robust fitting of the model in the presence of many data outliers. It is a non deterministic algorithm in the sense it produces reasonable result with a probability. This probability increases as more number of iterations are allowed. The goal is to determine the points in the space that projects onto an image into a set of landmarks with know location. The basic assumption is that the data consist of inliers i.e data whose distribution can be explained by some set of model. The outliers can come from extreme values of the noise from erroneous measurement or incorrect hypotheses about the interpretation of data. This is done in three steps 1.line fitting 2. Model fitting 3. Count inliers. Initially, 4 random features are selected following to that Homography H is calculated then inliers are computed. This is done for several iterations and the largest sets of inliers are recorded and H is recomputed using least square method. The output of RANSAC is a projective matrix and corresponding points between two images. Equation below represents the probability of at least 1 success after K trails.

$$\mathbf{P = 1 - (1 - p^n)^k} \quad .....(5)$$

Here, P = Probability of at least 1 success after K trail.
p = Probability of real inliers
n = Number of samples drawn each iteration.

The following equation [14] determines the number of iterations:

$$\mathbf{K = \log (1-P) / \log(1-p^n)} \quad .....(6)$$

Below is a table showing the value of K at P = 0.99 and various other values of n and p.

n	p	k
3	0.5	35
6	0.6	97
6	0.5	293

TABLE 1: Parameters for RANSAC .

6.3 Correspondence Point Filter – Distance Threshold

Harris corner detection has given the interest points in the images taken from different point of view. Randomized Search Algorithm (RANSAC) is now used to do the initial matching of the interest points which are identified as same in both the images. Next step is to determine the transformation matrix between two images. Before that it is important to eliminate false Interest points for better accuracy. This is done by using the distance threshold parameter in RANSAC. For an interest point to be accepted, its distance predicted by the transformation should not exceed the threshold "Distance threshold". This Threshold is used to check for the transformations consistency and it depends on the image acquisition method. In our case the images are acquired in a straight line along horizontal and vertical direction with all most same overlapping region.

6.4 Rigid Transformation

Rigid transformation preserves the shape and size in contrast to affine transformation, which includes shear and scaling also. Let us consider two data set A & B [15].

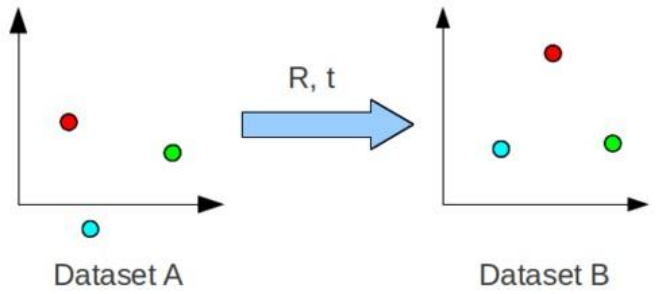

FIGURE 5.

In order to align set A on the Set B, Solution for rotation R and Translation T is calculated using equation 7.

$$\mathbf{B = R*A + T} \quad \text{.....(7)}$$

Following steps are carried out to find the most optimum rigid transformation.

6.4.1 Calculate the centroid of both data set.

Centroid are the average of all the points. It can be represented as :

$$P = \begin{bmatrix} x \\ y \end{bmatrix} \qquad centroid_A = \frac{1}{N}\sum_{i=1}^{N} P_A^i$$

$$centroid_B = \frac{1}{N}\sum_{i=1}^{N} P_B^i$$

Here P^i_A and P^i_B are points in the data set A and data set B.

6.4.2 Translate the data set to the origin and then find the rotation matrix R.

The Singular value decomposition (SVD) [16] is used to calculate the rotation matrix. SVD says that a rectangle matrix A can be broken down into the product of three matrices - U as orthogonal matrix, S as a diagonal matrix, and V as transpose of an orthogonal matrix. It is based on the theorem from linear algebra i.e

$$A_{mm} = U_{mm}\, S_{mm}\, V_{mm}^{T}$$

Here, $U^TU = 1$, $V^T V = 1$ and the column of U are orthogonal eigen vectors of AA^T. The column of V are orthonormal eigen vectors of A^TA, and S is the diagonal matrix with square root of eigen values from U and V in descending order. Now using SVD, Matrix H is computed.

$$H = \sum_{i=1}^{N} (P_A^i - centroid_A)(P_B^i - centroid_B)^T$$

$$[U, S, V] = SVD(H)$$

$$R = VU^T$$

In the above expression H is a covariance matrix of 2x2 order. In some special cases SVD will return reflection matrix. This is numerically correct but impractical in real world. This can be checked by calculating the determinant of V. if the determent is negative then -1 is multiplied to the 3rd column of the V.

6.4.3 Calculate translation

Translation can be found out by rearranging the equation 7 and plugging in the values of R, and Centroids of data set A & B.

$$t = -R * Centroid_A + Centroid_B \quad \text{.....(8)}$$

7. SKEW CORRECTION

The stitched image might have alignment issues in horizontal or vertical direction. This could be because of the incorrect calculation of the transformation matrix between image pairs with low or no texture. Skew error in 2D means lack of perpendicularity between two axes. By applying shear transformation (discussed in section 5.2) on the stitched image this error can be minimized. The transformation is applied either on the X-axis or on the Y- axis [17].

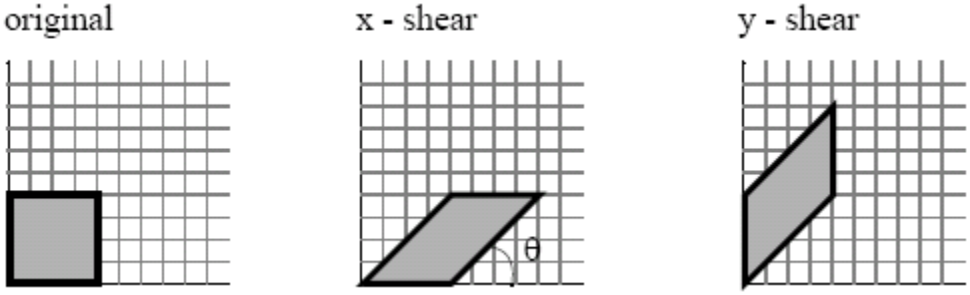

FIGURE 6(a) **FIGURE 6(b)** **FIGURE 6(c)**

Figure 6(b) and figure 6(c) represent possible type of shear in X and Y direction and Figure6 (a) represents a perfectly orthogonal image.

8. IMPLEMENTATION

In this section we will discuss about the practical implementation of Image Stitching. The algorithm was made with reference from various Hdevelop example programs. The algorithm was tested in a image processing software called as HALCON by MVTec. The specifications of the computer are 2GB RAM, 64 Bit Windows XP. Figure 7 represents a tiled image of 6 individual images of a PCB (These images are part of sample images from MVTec). The overlapping region was approximately 40%. Below is the flow chart for the program.

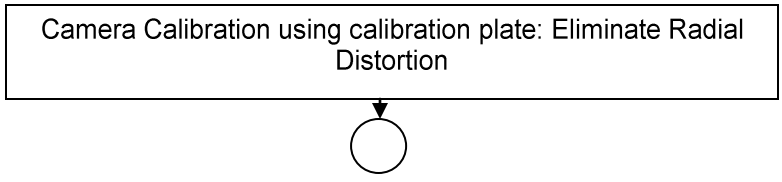

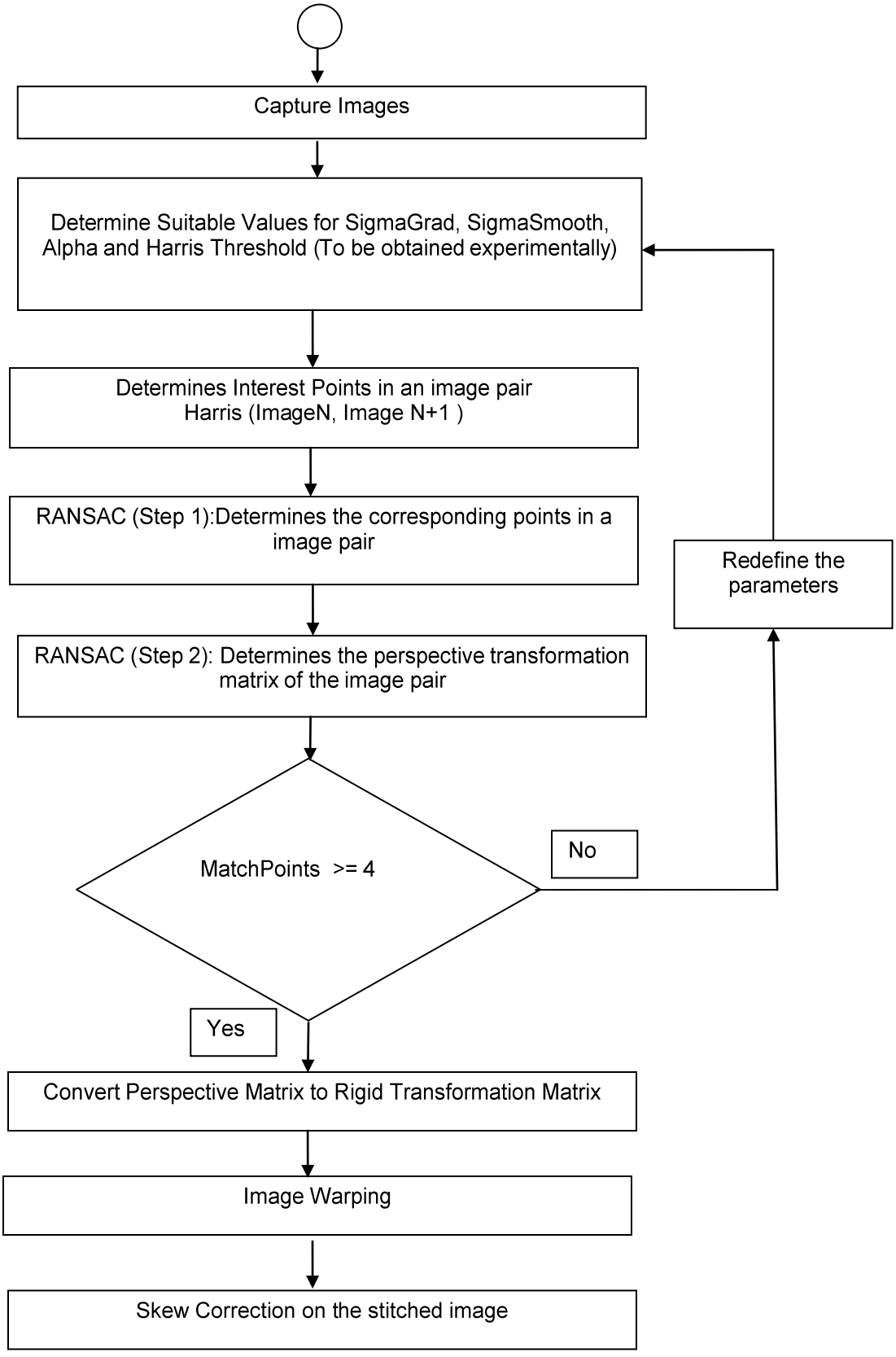
Capture Images
Determine Suitable Values for SigmaGrad, SigmaSmooth, Alpha and Harris Threshold (To be obtained experimentally)
Determines Interest Points in an image pair Harris (ImageN, Image N+1)
RANSAC (Step 1):Determines the corresponding points in a image pair
RANSAC (Step 2): Determines the perspective transformation matrix of the image pair
MatchPoints >= 4
No
Redefine the parameters
Yes
Convert Perspective Matrix to Rigid Transformation Matrix
Image Warping
Skew Correction on the stitched image

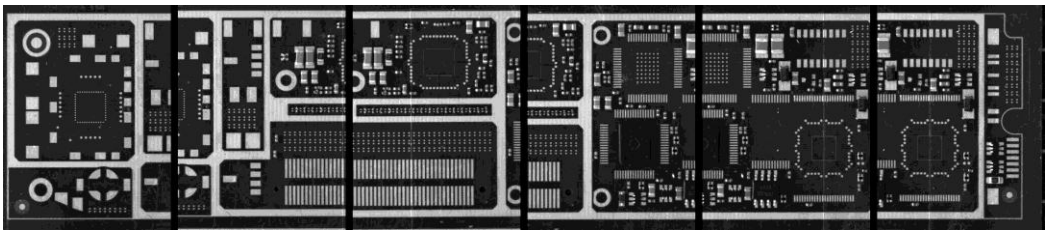

FIGURE 7: Tiled Images.

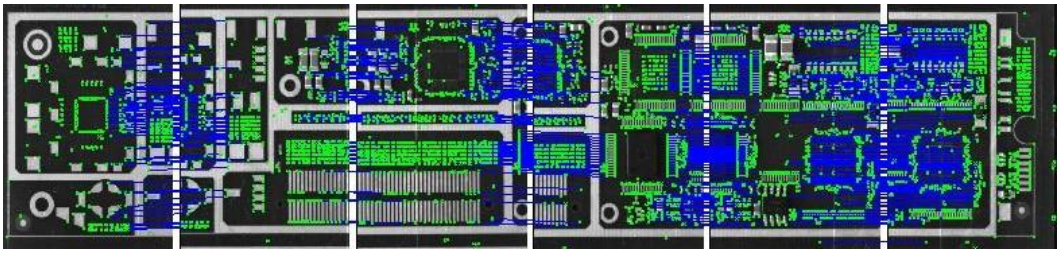

FIGURE 8: Interest Points and Correspondence points of tiled image.

Figure 8 has green points marked as unique interest points from Harris corner detection and blue lines are the corresponding points. Figure 9 is a Rigid Mosaic (before skew correction) of these 6 images. For each pair of image, rigid matrix was calculated and images were stitched. Figure 10 is the Stitched image after skew correction.

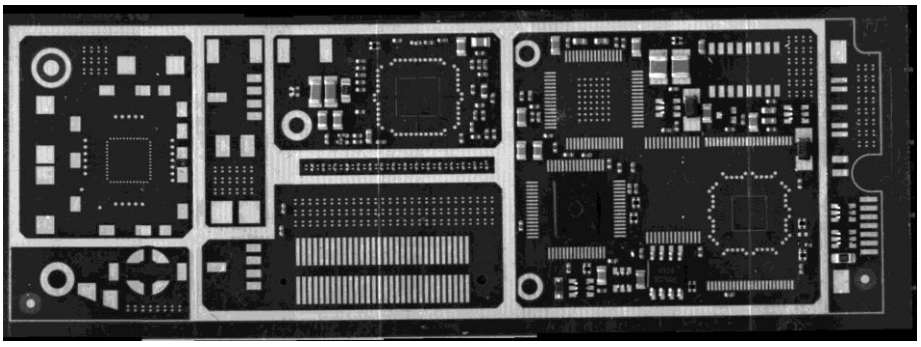

FIGURE 9: Stitched Image before skew correction.

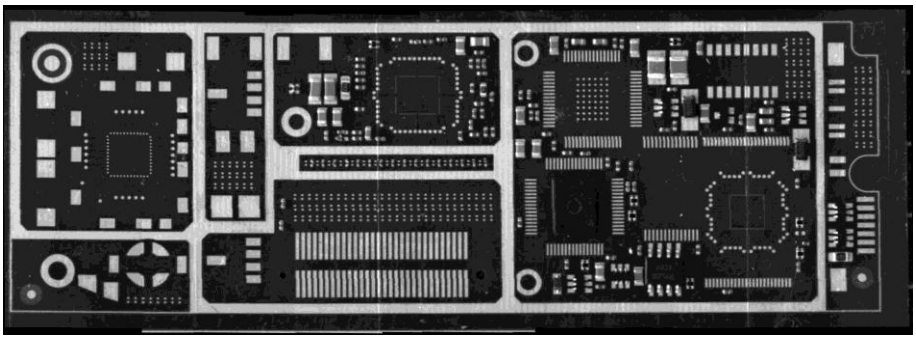

FIGURE 10: Stitched Image after Skew Correction.

9. LIMITATIONS AND DRAWBACK

Since the accuracy depended on imaging system and optics (telephoto lens). This makes the solution expensive and required huge space because of high working distance. Also, as the algorithm is completely interest points dependent minimum of 4 points are needed to accurately calculate the Homography Matrix. Failing to this will lead to unexpected mismatch in image stitching.

10. COMPARISON WITH OTHER MOSAICKING METHODS

Fan Zhang et al; In their research paper [18] have demonstrated a method in which homography is used to roughly align images first and then using content-preservation warping to fine tune the alignment followed by seam cutting and warping. This technique handles images with large parallax error but as mentioned in their paper, sometimes their stitched images suffer from noticeable perspective distortion. Jiaya Jia et al [19]; have proposed an approach based on structure alignment and deformation propagation in natural images. However their stitching algorithm may influence the stitching quality. Their algorithm highly depends on two factors i.e use of SIFT detector is not invariant to affine transformation and partial occlusion this may produce erroneous result, second is since the stitching is happening in the gradient domain there is no guarantee to produce the visual effects.

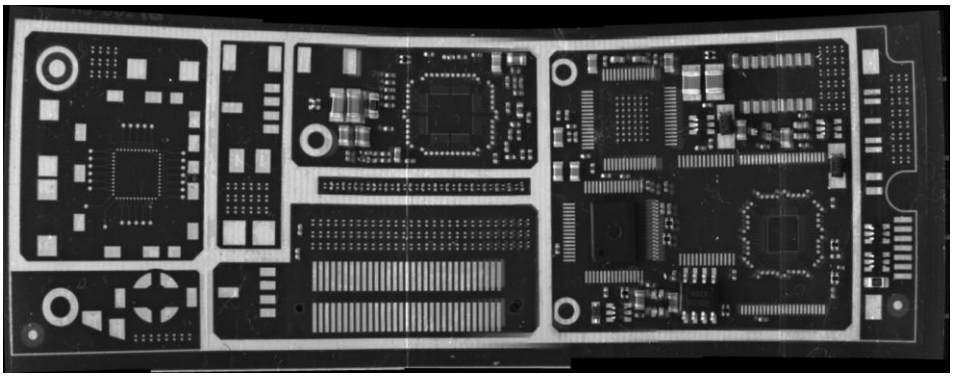

FIGURE 11: Stitched Image using autostitch software.

As there is no benchmark database available for PCB image stitching. We are comparing our results with autostitch software. From figure 11 it is very clear that there is an unexpected wrapping in the center of the image stitched by autostitch software. This disqualifies the image from extraction of CAD data.

11. CONCLUSION AND FUTURE WORK

This research provides a robust algorithm for Image stitching for any type of PCB. Following conclusion can be made from proposed research:

1. High Stitching Accuracy: Upon visual inspection of the stitched image there was no significant mismatch. One can expect accurate mosaic as long as images have texture in them.
2. Automatic Stitching: Once the initial parameters for Harris and RANSAC are identified for an image pair, then same parameters can be used for remaining set of image pairs.
3. Algorithm Speed: In order to speed up the algorithm the search area of the of the matching can be reduced.

Future work on this research involves reducing the mismatch error, making the optic system more cost effective and reducing the work space or working distance.

12. REFERENCES

[1] Vinod D.S and Vidhyallatha Prakash. " Intersity Based Image Mosaicing," 7th WSEAS international conference on Applied Computer science, Venice, Italy, Nov 21-23, 2007 Pg 111-116.

[2] V. Wyawahare, M. Patil and Abhyankar. "Image Registration Techniques: An overview," International journal of Signal Processing, Image Processing and Pattern Recognition Vol. 2,September 2009.

[3] MVTech Software GmbH. “3d Vision- HALCON Solution Guide 3C,” Munchen, Germany, July 2015, pp 69-100.

[4] Brown, Duane C. "Decentering distortion of lenses," Monthly Notices of the Royal Astronomical Society, Vol. 79, p.391.

[5] DCB Automation, “An Introduction to AOI, ” www.dcbautomation.com/wp-content/uploads/2014/09/1-Introduction-to-AOI.pdf [July 2015].

[6] MVTech Software GmbH. “Uncalibrated Mosaicking,” in book 3d Vision- HALCON Solution Guide 3C Edition 7A, Munchen, Germany, July 2015, pp 247-261.

[7] S.Widnal. “Vector, Matrices & Coordinate transformations,” http://ocw.mit.edu/courses/aeronautics-and-astronautics/16-07-dynamics-fall-2009/lecture-notes/MIT16_07F09_Lec03.pdf [June 2015].

[8] Don Fussell. “Affine Transformation,“ https://www.cs.utexas.edu/~fussell/courses/cs384g/lectures/lecture07-Affine.pdf [June 2015].

[9] C.Schmid, R.Mohr & C.Bauckhage. “Evaluation of interest points detector,” International Journal of Computer Vision 37(2):151-172, June 2000.

[10] C.Harris & M.J. Stephens. “A Combined Corner & Edge Detector,” In Alevey Vision Conference pp 147-152, 1988.

[11] H. Moravec. “Obstacle Avoidance and Navigation in the real world by a seeing robot rover,” Technical Report CMU-R1-TR-3, Carnegie-Mellon University, Robotics Institute, 1980.

[12] HALCON MVTec, "Points Harris," www.halcon.com/download/reference/points_harris.html. [Sept 2015].

[13] Martin A, Fischler & Robert C. Bolles. “ Random sample consensus: a paradigm for model fitting with applications to image analysis and automated cartography,” Magazine communications of ACM, Vol 24 Issue 6 June 1981.

[14] “Multiview Geometry in Computer Vision”, Cambridge Universal Press, pp119.

[15] Nghia ho, “ Singular value decomposition,” www.nghiaho.com/?attachment_id=675 [15 Jan 2016].

[16] Kirk Baker. “Singular Value Decomposition Tutorial,” March 29, 2005 (Revised January 14, 2013).

[17] Foley & Van Dam. “ 2D Geometric Transformation,” http://www.cs.brandeis.edu/~cs155/Lecture_06.pdf[June 2015].

[18] Fan Zhang and Feng Liu. “Parallax Tolerant Image Stitching,” IEEE Conference on Computer Vision and Pattern Recognition, Columbus,OH, 23-28 June 2014, Pg 3262 - 3269.

[19] Jiaya Jia, Chi-Keung Tang. “Image Stitching Using Structural Deformation,” IEEE Transaction on pattern analysis & machine intelligence Volume 20, No.4, April 2008.